Scalar turbulence

Boris I. Shraiman* **& Eric D. Siggia†**

** Bell Laboratories, Lucent Technologies, Murray Hill, New Jersey 07974, USA*
† Center for Physics and Biology, Rockefeller University, New York, New York 10021, USA

The advection of a passive substance by a turbulent flow is important in many natural and engineering settings. The concentration of such a substance can exhibit complex dynamic behaviour that shows many phenomenological parallels with the behaviour of the turbulent velocity field. Yet the statistical properties of this so-called 'passive scalar' turbulence are decoupled from those of the underlying velocity field. Passive scalar turbulence has recently yielded to mathematical analysis, and such progress may ultimately lead to a better understanding of the still intractable problem of fluid turbulence itself.

The concentration of a substance advected by a turbulent flow exhibits a complex, chaotically evolving structure over a broad range of space and time scales. The "substance" could be a pollutant, as in the familiar case of smoke dispersing in air; it could be heat, when a hot object is cooled in the flow; or (as in Fig. 1) a fluorescent dye mixed by a turbulent jet. Turbulent advection is important in many natural and engineering settings, ranging from atmospheric phenomena[1] and combustion[2] to the stretching and amplification of magnetic fields on both galactic and terrestrial scales[3]. It is even relevant in a biological context. For example, many organisms need to locate the sources of attractive odours: the chemotactic 'algorithms' by which this is achieved will differ according to whether the organism is in a diffusion-dominated world (as in the case of bacteria[4]) where local concentration gradients can be used to navigate, or in a turbulent world (like lobsters[5] or moths[6]) where large flow-induced fluctuations of the local concentration gradient render it useless for navigation. In many cases, the advected "substance" has a strong effect on the turbulent flow itself, by generating local forces: for example, non-uniform heating would act on the flow through buoyancy. However, the phenomenon of turbulent advection and mixing caused by it may be separated from the forces responsible for the flow.

Here we concentrate on the case where the advected substance is passive and so has a negligible back effect on the flow (this also applies to the temperature field if buoyancy forces are small compared to the inertial stresses driving the flow), and on situations of well controlled laboratory turbulence[7,8]. Given that the substances are passive and are described by scalar (rather than vector) fields, they all behave in the same way. Thus generically we speak of 'passive scalar' advection.

Turbulent flow transports and disperses the scalar by making parcels of fluid follow chaotic trajectories. The spatial non-uniformity of the velocity field causes the lines of constant scalar concentration to stretch and fold; as a result, variations of the scalar concentration reach progressively smaller scales. This process amplifies the local concentration gradients until molecular diffusivity finally takes over, causing local variations of the scalar to dissipate. The result of these processes is a dramatic acceleration of the rate of mixing which, for a fully turbulent flow, becomes independent of molecular diffusivity. However, the price of the (on average) rapid mixing is the frequent occurrence of large fluctuations of the scalar field, which are quantified by departures of the probability distribution functions (PDF) of the scalar field from gaussian behaviour[8,9]. Turbulent mixing, defined as the dissipation of scalar variance, is "intermittent"[7,9,10]—it occurs in spatio-temporal bursts qualitatively similar to the energy dissipation by the turbulent velocity field itself. Although the dynamics of the underlying velocity (vector) field is intrinsically nonlinear and much more complex to describe, there are so many parallels between the statistics of the scalar fluctuations and those of turbulent velocity that one may justifiably refer to the behaviour of the advected scalar as 'scalar turbulence'. The basic understanding of turbulent mixing and transport emerged through the work of Taylor, Richardson, Kolmogorov, Obukhov and Corrsin (as reviewed by Monin and Yaglom[11]). However, while their simple dimensional arguments[11,12] are successful in explaining the average rate of spreading or mixing of, say, a smoke plume, understanding the statistics of the large fluctuations is a more difficult problem. We will address this below.

The practical relevance of understanding the statistics of large fluctuations is obvious if one considers, for example, the probability of a pollutant concentration exceeding some tolerable level as it spreads from a source. More subtle, but equally important, is the role of large concentration fluctuations in controlling the rate of slow (high order) chemical reactions, for example in the process of atmospheric ozone destruction[13].

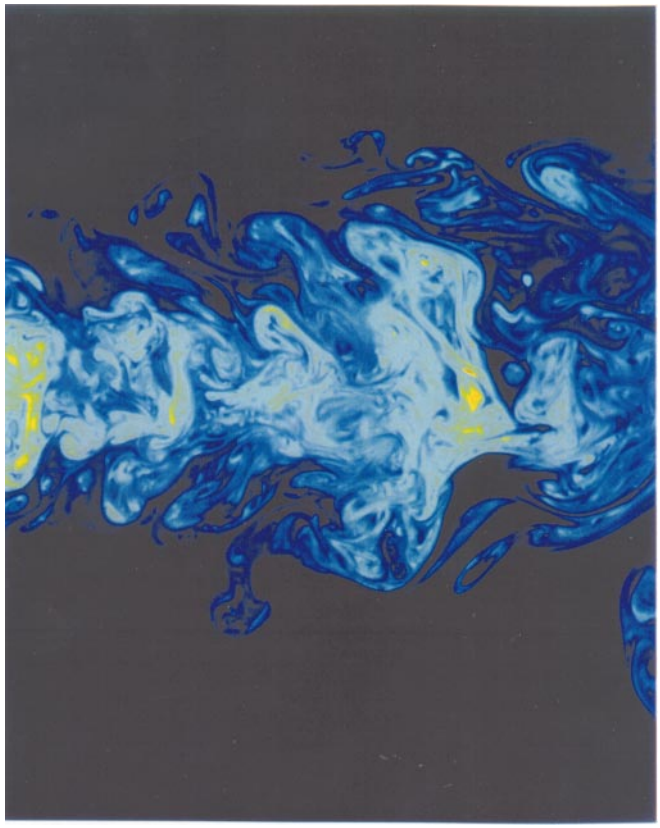

Figure 1 Fluorescent dye in a turbulent jet. The Reynolds number, Re, is 4,000 (K. R. Sreenivasan).

This Review is prompted by recent progress in the statistical description of passive scalar turbulence. Central to this progress has been the realization that anomalous scaling properties and the appearance of coherent structures in the scalar field—well known characteristics of fluid turbulence itself—occur even for a scalar advected by a simple random gaussian velocity field (which resembles real turbulence only in the way the fluctuations are distributed over small spatial scales[14–17]). The non-trivial statistical aspects of the scalar turn out to originate in the mixing process itself, rather than being inherited from the complexity of the turbulent velocity field. Study of passive scalar turbulence is therefore decoupled from the still intractable problem of calculating the velocity statistics, and so has yielded to mathematical analysis[18–20]. Conversely, the well established phenomenological parallels between the statistical description of mixing and fluid turbulence itself[9,10] suggest that progress on the latter front may follow from a better understanding of turbulent mixing.

Observations and phenomenology

The simplest characterization of turbulent mixing is through a local measurement of the advected field. Measurements of temperature at a given point in a turbulent flow—for example, on the axis of a hot jet mixing with a cold bath[21] or within a turbulent boundary layer over a heated surface[22,23]—are typical of many laboratory experiments. Closer to the idealized case of 'homogeneous and isotropic' turbulence are the recent studies by Warhaft and co-workers[24,25], in which temperature fluctuations were measured behind the grid in a wind tunnel where the inlet flow was preheated to impose a linear temperature profile (in a direction transverse to the flow). In all of these cases, the temperature measured downstream from the inlet as a function of time, $\Theta(t)$, fluctuates about its mean value $\langle\Theta(r)\rangle$ at the point of observation r as parcels of colder or warmer fluid sweep by. The fluctuations are then quantified by constructing, from the temporal sequence, a histogram or PDF, $P(\Theta)$. If the scalar field is injected randomly[11], the resulting single-point PDF is gaussian. In the more common case when the 'injection' produces a large-scale temperature gradient[24,26], a regime of exponential tails (see Fig. 2a) is observed. In either case, the root-mean-square (r.m.s.) fluctuation is of the same order of magnitude as the temperature variation on the scale characteristic of the flow as a whole—the so-called 'integral scale', which is set by the geometry (for example, the jet diameter or wind tunnel grid).

Another important observable is the difference between simultaneous measurements at two points separated by a distance r, expressed as $\Delta_r\Theta \equiv \Theta(x+r,t) - \Theta(x,t)$. The PDF of the difference is shown in Fig. 2b: it starts as a gaussian for point separations of the order of the integral scale L, and evolves progressively longer exponential or stretched-exponential tails as r decreases towards the dissipation scale η, where the scalar difference can be approximated by a derivative. This excess of large fluctuations (compared to a gaussian distribution) on small scales, termed 'intermittency', is well known for the statistics of the velocity fluctuations themselves $(\Delta_r v)$[9,10].

The behaviour of the scalar field is determined by two physical effects: (1) transport, the physical translocation of impurities or heat by the combined action of the flow and diffusion; and (2) mixing, the irreversible decay of fluctuations, ultimately due to the molecular diffusivity, κ, which (in the absence of forcing) will tend to reduce the scalar field to uniformity. In turbulent flow, both the transport and mixing rate become independent of κ when the diffusivity is infinitesimally small. (The latter limit is highly non-trivial because diffusivity, no matter how small, dominates over advection by the flow at sufficiently small scales and expresses the irreversibility of molecular mixing.)

Taylor proposed[12] that the motion of a single particle in turbulent flow is diffusive, and given by $\langle R^2(t)\rangle \sim D_{\rm eff}t$ (where $R(t)$ is the particle displacement in the reference frame moving with the mean flow velocity) with the effective diffusivity of the order of $D_{\rm eff} \approx \Delta V^2\tau_L$ (where ΔV is the r.m.s. velocity fluctuation at a point, and τ_L is the velocity correlation time). As the correlation length of the velocity field is the integral scale L, the correlation time τ_L is estimated dimensionally as $L/\Delta V$, and the effective diffusivity $D_{\rm eff}$ turns out to be independent of κ.

Single-particle diffusion must be contrasted with the dispersion of nearby particles, which also governs the spreading of the 'plume' that appears when the scalar is injected locally. According to Richardson[12], the relative motion of a pair of particles with separation $r < L$ is governed by $\langle r^2(t)\rangle \sim \epsilon t^3$, where $\epsilon \approx \Delta V^2/\tau_L$ is the energy dissipation rate for the turbulent velocity field[10,12]. Richardson's law only holds for short times (while $r \leqslant L$), but does predict that two particles will separate to the integral scale in a time independent of their initial separation. Although according to Richardson r^2 grows as a power of t rather than linearly, in fact the particles are separating more slowly than they would under Taylor diffusion (note that $\epsilon \sim D_{\rm eff}/\tau_L^2$). This happens because the motion of particles within an integral scale of each other is correlated. For $\tau > \tau_L$ and $r > L$, particles decorrelate and Richardson's law crosses over to Taylor's law. In fact, Richardson's law is obtained by assuming relative motion to be diffusive but with a diffusion constant $D(r) \sim \epsilon^{2/3}r^{4/3}$ which increases with r. This behaviour follows from Taylor's argument once one takes into account that the variance of the (relative) velocity fluctuations on scale r is $\langle(\Delta_r v)^2\rangle \sim \epsilon^{2/3}r^{4/3}$ and the corresponding correlation time is $\tau_r \approx r/\Delta_r v \sim \epsilon^{-1/3}r^{2/3}$. The last two expressions are the predictions of Kolmogorov's 1941 (K41) scaling theory[10].

Kolmogorov's theory[10] postulates the following: (1) the energy dissipation rate ϵ is independent of the viscosity ν provided that the Reynolds number $\mathrm{Re} = \Delta VL/\nu$ is sufficiently large (that is, when

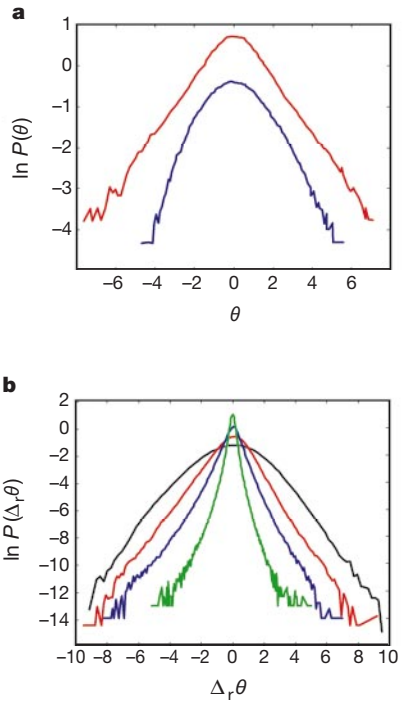

Figure 2 Probability distribution functions (PDF). **a**, $P(\theta)$ 62 grid lengths downstream in a wind tunnel with (blue) and without (red) a mean gradient (from ref. 24); the scalar field θ is scaled to unity for each curve. **b**, The PDF of scalar difference $\Delta_r\theta$ at different separations starting from the integral scale $r = 230\eta$ (black), through to the inertial range $r = 96\eta$ (red), 26η (blue) and 6.5η (green) (from F. Moisy, W. Herve and P. Tabeling, manuscript in preparation). Note that the r.m.s. decreases with decreasing scale but the fluctuations that are large compared to the r.m.s. become more likely as the PDFs evolve from gaussian on the integral scale to a stretch-exponential on small scales.

inertial forces dominate over viscous forces); (2) ϵ is the *only* relevant parameter which controls turbulent fluctuations on scales $r \ll L$. The first postulate has strong experimental support, as does the aforementioned 2/3 law for the velocity variance as a function of r (refs 9–12). Kolmogorov's argument was extended to passive scalar by Obukhov and Corrsin[11]. The Kolmogorov–Obukhov–Corrsin theory states that the dissipation rate of scalar variance[11,12], $\epsilon_\Theta \equiv -\mathrm{d}/\mathrm{d}t\langle(\Delta\Theta)^2\rangle$, is independent of molecular diffusivity and is set by the large eddy turnover rate τ_L^{-1}, so that $\epsilon_\Theta \sim \langle(\Delta\Theta)^2\rangle/\tau_L$. Because dissipation occurs only on small scales, the same scalar variance flux must pass through the 'inertial range' comprising all scales intermediate between the initial injection scale L and the final dissipation scale η (see below). Using the K41 estimate for $\Delta_r v$ on scale r, one obtains $\langle(\Delta_r\Theta)^2\rangle \sim \epsilon_\Theta \epsilon^{-1/3} r^{2/3}$. Molecular diffusivity enters only in setting the scalar dissipation scale η by matching the dissipation rate defined by $\kappa\langle(\Delta_\eta\Theta/\eta)^2\rangle \sim \epsilon_\Theta$.

Kolmogorov–Obukhov–Corrsin (KOC) theory also predicts simple scaling for the time average of higher powers of $\Delta_r\Theta$, (the moments of the PDF) or the so-called structure function, $S_{2n}(r) \equiv \langle(\Delta_r\Theta)^{2n}\rangle \approx \langle(\Delta_r\Theta)^2\rangle^n$. Therefore a universal PDF of scalar differences is predicted, $P(\Delta_r\Theta/\langle(\Delta_r\Theta)^2\rangle^{1/2})$, where all the dependence on the measurement scale is accounted for by normalizing to the r.m.s. of the fluctuations. Although the KOC prediction for the second moment is close to experimental values[7,8], its predictions for the high moments are far off: as evident from the strong dependence of the shape of the difference PDF on scale r, Fig. 2b. The non-Kolmogorov behaviour of large fluctuations can be quantified by the observed[8,9] anomalous scaling of the moments: $S_{2n}(r)/S_2^n(r) \approx (r/L)^{\zeta_{2n}-2n/3}$. The deviation of the scaling exponents ζ_{2n} from their KOC values $(2n/3)$ are even larger than those known for the velocity structure function[9,10], indicating that the intermittency in the scalar field is even stronger. The anomalous scaling means that ϵ_Θ (like ϵ in the K41 theory) is not the only relevant parameter for $r < L$. On purely dimensional grounds, the integral scale L must enter inertial range quantities. However, there is no unique definition of L and numerically any expression for L will reflect the anisotropy of the large scales. Is it even possible that the small scales are anisotropic, imprinted by the anisotropies on the large scales, and therefore quite non-universal? The definitive answer is still not known, yet the study of the passive scalar problem sheds light on the mechanism that could apply to the velocity as well.

Before returning to the failure of the K41 theory in describing the fluctuations, we will look further into the physics underlying the remarkable and correct first postulate: the independence of the dissipation rate on the viscosity and molecular diffusivity κ. Consider first a passive scalar in a random flow characterized by single length and time scales, L and $\tau_L \approx \Delta V/L$, respectively. The characteristic magnitude of the velocity gradient in this so-called Batchelor flow regime is $\gamma = \Delta V/L$. A scalar blob will be stretched and rolled up by the flow and, because of the incompressibility, acquire structure—such as tendrils and 'Swiss roll' shapes—on progressively smaller scales $l(t) \approx L\exp(-\gamma t)$. Molecular mixing occurs rapidly and gradients disappear at the time t_*, when the folds of the scalar field reach down to the scale where the diffusion rate becomes comparable to the rate of stretching, $\kappa/l^2(t_*) \approx \gamma$. This defines the dissipation scale for Batchelor flow expressed as $\eta_B \approx L/\mathrm{Pe}^{1/2}$, which depends on κ through the Peclet number $\mathrm{Pe} \equiv \Delta VL/\kappa \gg 1$ and the mixing time $t_* \approx \gamma^{-1}\ln \mathrm{Pe}$ which is

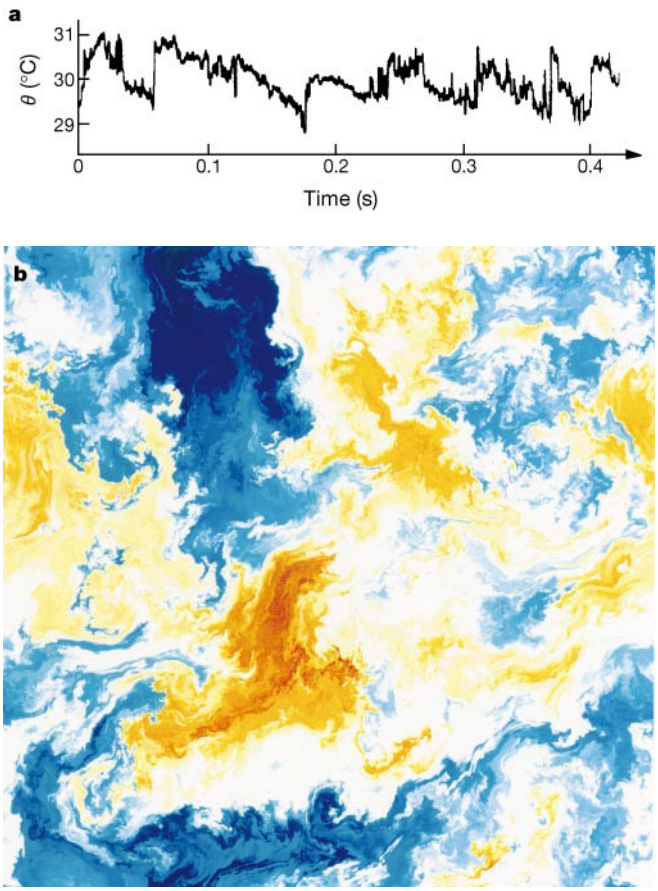

Figure 3 Scalar fluctuations in time and space. **a**, Temporal trace of the temperature recorded at a fixed point in a turbulent boundary layer over a heated plate from ref. 23. Note the asymmetry of the derivative. **b**, Numerical simulation of passive scalar advection in two dimensions for the Kraichnan model with velocity defined by equation (2) and $\gamma = 0.5$ on a 8192 square grid[31]. The concentration scale runs from blue to red.

only weakly (logarithmically) dependent on κ. The rate of mixing and scalar dissipation follows t_*^{-1}. (This argument tacitly assumes the flow to be sufficiently random not to be concerned with the possible existence of stagnation points, separatices and subregions left invariant by the flow. Their appearance is possible in weakly time-dependent (single-scale) flows even when trajectories on average separate exponentially. The latter is the case for chaotic advection which is an important instance of mixing[27,28] in its own right. Realization of Batchelor's random flow limit has been plausibly achieved in several experiments[29,30], although observation of Batchelor's scaling[12] remains elusive.)

In contrast to the Batchelor regime, flows at high Re number involve not one but many length scales. But the above argument can be used on each octave of scales (starting with the dissipation scale η, for example, $l \approx \eta, 2\eta, 4\eta, \ldots L$) and the mixing times sum to a constant ($\sim\tau_L$) independent of κ by virtue of the Kolmogorov expression for τ_r. Thus a multi-scale flow acts as if it had an effective diffusivity, $\kappa_{\rm eff} \approx D_{\rm eff} \sim \Delta VL$. However, the latter interpretation is consistent with observation only for the averaged scalar dissipation. Large fluctuations of the dissipation rate reveal a breakdown of the 'effective diffusivity' view of mixing, and may be attributed to patchiness of the process where intermediate scales become transiently quiescent, leaving the mixing of large variations of the scalar entirely to the small-scale velocity. K41 'cascade' type theory does not tell us what these fluctuations are.

In turbulence theory, the discussions of intermittency and of the consequent deviations from K41 scaling often invoke the presence of "coherent structures"—for example, vortex filaments—amidst turbulent fluctuations[9,10]. For the scalar, the excess (relative to K41) fluctuations on small scales and associated anomalous scaling exponents, as well as fluctuations of the local rate of mixing, can all be interpreted in terms of the structures revealed in experimental traces such as that shown in Fig. 3a. The saw-tooth appearance is indicative of a field organized into a transient array of plateaux, up to L in size, separated by sharp cliffs[22,23]. (The scalar in Fig. 3a is constrained to have zero mean, which converts the plateaux to ramps). Remarkably, such events are sufficiently common (roughly one per integral scale and turnover time) that the normalized odd moments $S_{2n+1}(r)/S_2^{n+1/2}(r)$ which according to the K41 isotropization hypothesis should tend to zero as $(r/L)^{2/3}$ with decreasing r (or as $\mathrm{Re}^{-1/2}$ for the corresponding derivative ratio) do so very slowly and possibly not at all[7,23,25].

Furthermore, numerical simulations[16,17,31] have shown most decisively that the 'structures' in the scalar are not mere footprints of organized vorticity in shear flow, but are intrinsic to mixing. In the numerical simulation the velocity field is a structureless, artificial, gaussian process, yet the plateaux and cliff structures are clearly evident (Fig. 3b). The mechanism is intuitively appealing: turbulent mixing effectively expels whatever large-scale gradient there is, forming patches of nearly constant scalar field which are reconciled with the existing large-scale gradients by the formation of fronts (that is, intense gradient sheets).

Contrary to effective diffusivity notions, the sheets are sharp, and form transiently in the vicinity of the hyperbolic points of the large-scale flow (Fig. 7 of ref. 16) where 'jets' carrying high and low values of the scalar collide. Large and small scales are thereby directly coupled, producing large fluctuations on small scales and dominating high moments of the scalar structure function. If a static large-scale gradients is imposed, the fronts preferentially align normal to its direction and a violation of small-scale isotropization (for example, an anomalously large third order moment) is produced as well, so that odd moments computed numerically agree with experiment[16,17]. The remarkable lesson here is that intermittency in scalar mixing is intrinsic, decoupled from that in the velocity field, and approachable via the simpler problem of advection by random flow pioneered by Batchelor[12] and Kraichnan[14,15]—which we shall discuss next.

Kraichnan's model

Scalar transport and mixing is described by the following advection/diffusion equation:

$$\partial_t \Theta(\boldsymbol{r},t) + \mathbf{v}(r,t)\cdot\boldsymbol{\nabla}\Theta(\boldsymbol{r},t) = \kappa\boldsymbol{\nabla}^2\Theta(\boldsymbol{r},t) \qquad (1)$$

where Θ is the scalar field (that is, temperature or dye concentration), $\mathbf{v}(\boldsymbol{r},t)$ is the velocity field, and κ is molecular diffusivity. In the absence of direct sources in the bulk of the fluid (which is often the case), the scalar is driven by external boundary conditions, which impose a time independent average $\langle\Theta(\boldsymbol{r})\rangle$. We are interested in the deviations from this average, the fluctuations $\theta(\boldsymbol{r},t) \equiv \Theta(\boldsymbol{r},t) - \langle\Theta(\boldsymbol{r})\rangle$. Rewriting equation (1) in terms of $\theta(\boldsymbol{r},t)$ we find on the right-hand side an additional term $s(r,t) \equiv -\mathbf{v}(\boldsymbol{r},t)\cdot\boldsymbol{\nabla}\langle\Theta(\boldsymbol{r})\rangle$: the gradient forcing.

Alternatively, as a mathematical expedient, equation (1) can be considered with a gaussian random source. In reality, the velocity field is governed by the Navier–Stokes equation as appropriate to the experiment or natural phenomenon at hand. However, in the passive scalar model we replace real turbulent flow by an incompressible random velocity field, which Kraichnan[14,15] took to be gaussian and δ-correlated in time. The velocity ensemble is then fully specified by the two-point correlator[14]:

$$\langle v_a(r,t)v_b(0,t')\rangle - \langle v_a(0,t)v_b(0,t')\rangle = D_{ab}^{(\gamma)}(r)\delta(t-t') \qquad (2)$$

where the magnitude of the symmetric tensor $D_{ab}^{(\gamma)}(r)$ varies as $\sim|r|^{2-\gamma}$ and the dependence on the spatial indices ensures the incompressibility (that is, $\partial_r^a D_{ab}^{(\gamma)}(r) = 0$). The averaging denoted by $\langle\ldots\rangle$ is over the gaussian velocity ensemble. The two parameters of the model are the scaling index γ and (as the mathematical problem is well posed in space of any dimension greater than 1) the spatial dimension d, which will prove very useful analytically. To make contact with physical flows which have finite and scale-dependent correlation time $\tau(r)$, one compares $\int \mathrm{d}t\langle(v(r,t)-v(0,0))^2\rangle$ with the (lagrangian) relative diffusivity of particles. Thus Richardson $r^{4/3}$ scaling of the relative diffusivity $D_{\rm eff}(r)$ is recovered for $\gamma = 2/3$. The Batchelor, single-scale flow, limit is described by $\gamma \to 0$ and a 'rough' (non-differentiable) velocity field by $\gamma \to 2$.

Despite the relative simplicity of equations (1) and (2), the statistics of the scalar field is highly non-trivial. Kraichnan demonstrated in 1968 (ref. 19) that these equations lead to $\langle(\theta(\boldsymbol{r},t)-\theta(0,t))^2\rangle \sim r^\gamma$, and thus, for $\gamma = 2/3$, consistency with KOC. Yet, he later surmised[15] that all higher (even) moments of the scalar difference exhibit anomalous scaling and thus that the model equations (1, 2) also capture scalar intermittency.

The lagrangian view of mixing

The effect of advection (the $\mathbf{v}\cdot\boldsymbol{\nabla}\theta$ term in equation (1)) can be dealt with mathematically by changing from the laboratory (or eulerian) coordinate system to lagrangian coordinates, which follow material elements in the flow. The diffusion term in these moving coordinates would appear intractable but, thanks to the linearity of the equation, the effect of diffusion may be correctly represented by including brownian motion in the lagrangian dynamics:

$$\frac{\mathrm{d}}{\mathrm{d}t}\theta(t) = s(\boldsymbol{\rho}(t),t) \qquad (3)$$

$$\frac{\mathrm{d}}{\mathrm{d}t}\boldsymbol{\rho}(t) = \mathbf{v}(\boldsymbol{\rho}(t),t) + \boldsymbol{\eta}(t) \qquad (4)$$

where $\theta(t)$ is the scalar concentration of the fluid element presently at position $\boldsymbol{\rho}(t)$ and $\boldsymbol{\eta}(t)$ is the Langevin noise $\langle\eta_a(t)\eta_b(t')\rangle = \kappa\delta_{ab}(t-t')$ (introduced to represent the diffusion). In the absence of sources, θ is conserved along each trajectory, but the scalar field at the observation point r at time t is an average over

all the trajectories of the Langevin ensemble. The field at time t is related to the field at an earlier time t' by:

$$\theta(r,t) = \int \mathrm{d}r' G(r,t|r',t')\theta(r',t') \qquad (5)$$

with the Green's function representing the probability of trajectory (described by equation (4)) leaving from point r' at t' to arrive at r, t given by a path integral[32–35]:

$$G(r,t|r',t') = \int_{\rho(t')=r'}^{\rho(t)=r} D\rho \exp\left[-\frac{1}{2\kappa}\int_{t'}^{t}\mathrm{d}t''(\dot{\rho}-v(\rho,t''))^2\right] \qquad (6)$$

The most likely trajectory arriving at the observation point (r, t) is the one which makes the 'action', in the exponent of equation (6), vanish. This zero-action path is exactly the deterministic lagrangian (L) trajectory governed by equation (4) without the Langevin noise. For short elapsed time $t - t'$, the action localizes these trajectories close to the L-trajectory so that equation (5) picks out the lagrangian pre-image of the observation point and equates the observed $\theta(r, t)$ to the θ of the pre-image. At longer times, the kernel G in equation (5) samples increasingly larger and larger volume of r', making the observed $\theta(r, t)$ an average over the initial field and therefore decreasing its variance. This is how dissipation is represented by the path integral.

Having introduced the Green's function in equation (6), we construct a formal solution of equation (1) with sources which generalizes equation (5),

$$\theta(r,t) = \int_{-\infty}^{t}\mathrm{d}t' \int \mathrm{d}r' G(r,t|r',t')s(r',t').$$

The path integral lends itself to a semiclassical approximation: the transition probability expressed in equation (6) is dominated in the $\kappa \to 0$ limit by classical, minimal action trajectories (governed by the Euler–Lagrange equation) each contributing with the probability given by $\exp(-A_c/\kappa)$, A_c representing the action on the classical trajectory. For large $t - t'$, the classical trajectories diverge exponentially with the Lyapunov exponent (which measures the average rate of divergence) depending on the history of velocity gradient traversed by the L-trajectory. When the r' integral in equation (5) extends over a region much larger than the integral scale, the contribution of the sources self-averages, effectively cutting off the t' integral and defining a characteristic time for which the 'memory' of the sources persists. The latter quantity (on average) coincides with the mixing time t_*, but for each trajectory it depends on the velocity field in a well defined way enabling a quantitative analysis of the fluctuations.

The semiclassical approximation was used in ref. 35 to calculate the exponential tails in the single-point PDF $P(\theta)$ in the presence of a θ-gradient uniform over scales $\gg L$. Although the transport process between regions of size $\sim L$ is a random walk, large excursions in θ can occur for fluid parcels subject to little mixing. This is controlled by the trajectory-averaged Lyapunov exponent and, assuming gaussian statistics of $v(r, t)$, one can show that the probability distribution of mixing times is exponential[35]. The exponential tails of $P(\theta)$ follow, in agreement with experiments[24,26]. A δ-correlated velocity model is not a compromise with reality for processes that naturally occur on times much longer than the integral time τ_L, as is the case here. The tails of $P(\theta)$ can matter in practical problems. Consider the average rate of a thermally activated process (energy Δf) $\int \mathrm{d}\Theta \exp(-\Delta f/k_B\Theta)P(\Theta)$ or the probability that the pollution level exceeds some norm as it spreads from a source. A gaussian versus exponential distribution make very different predictions for the probability of rare events.

The statistical properties of $\nabla\theta$ may be computed in a similar fashion (in the Batchelor limit)[35–37]. The key difference is that the gradient is amplified by the action of the strain along the path. This amplification is again controlled by the Lyapunov exponent along the L-trajectory, and thus is in direct competition with dissipation acting through divergence of nearby paths expressed in equation (5). The PDF of the scalar dissipation $P(\nabla\theta)^2)$ and the statistics of the Lyapunov exponents are discussed in refs 36 and 37 and can be compared with experimental data[38].

Multi-point correlators

Further information about the fluctuating scalar field may be obtained by studying multipoint correlators, $C_N = \langle\theta(r_1,t)\theta(r_2,t)\ldots\theta(r_N,t)\rangle$ which involve simultaneous measurements of the field at N points. Unlike the traditional two-point structure function, $S_N(r)$, these objects contain not only the information about scaling properties but, through their dependence on the configuration of the measurement points, also probe the spatial structure of relevant fluctuations. Remarkably, these multipoint correlators also provide a convenient point of departure for the mathematical description of scalar statistics. An explicit path integral expression relating $C_N(t)$ to its value at earlier times follows readily from equations (5) and (6), but it is even more useful to consider evolution over very short times. For Kraichnan's δ-correlated model given in equation (2) the latter may be expressed in a differential form[14,35]:

$$\partial_t\langle\theta(r_1,t)\ldots\theta(r_N,t)\rangle = H_N\langle\theta(r_1,t)\ldots\theta(r_N,t)\rangle + I_N(r_1,\ldots r_N,t) \qquad (7)$$

with the so-called 'Hopf' evolution operator:

$$H_N \equiv -\sum_{i\neq j}[D_{ab}^{(\gamma)}(r_i - r_j) + \kappa\delta_{ab}]\partial_i^a\partial_j^b \qquad (8)$$

where the pair diffusivity $D_{ab}^{(\gamma)}(r)$ defined in equation (2) appears upon performing the gaussian velocity average. The inhomogeneous source terms, $I_N(r_1,\ldots r_N, t)$, on the right-hand side depend only on the lower-order correlators ($N-2$ and $N-1$ for gradient forcing) so that equation (7) is a closed hierarchy which can be solved starting with $N = 2$. This equation was first written down and solved for $N = 2$ by Kraichnan[14]. Physically, the Hopf operator generalizes Richardson diffusion to many pairs of particles as they follow their lagrangian trajectories. Just as for ordinary diffusion, equation (7) is first order in time and second order in spatial derivatives. The same operator governs the evolution of a 'swarm' of N particles advected by random flow, and defines the transition probability from one configuration to another. The evolution operator H_N plays the role of the hamiltonian in the Schrodinger equation: this analogy with quantum mechanics is particularly evident in the path-integral representation.

In the presence of steady forcing, the correlators become stationary, the time derivatives vanish, and each C_N has to be determined in terms of the previous $C_{j<N}$ in the hierarchy by inverting the Hopf operator H_N. By analogy with the harmonic polynomials which solve $\nabla^2\psi = 0$ and are necessary to satisfy the boundary conditions in electrostatics, homogeneous solutions or zero modes, $H_N\Psi = 0$, have to be added to each order to satisfy the boundary conditions, where the inertial range solution is matched to the large-scale flow. Thus the general solution has this form:

$$C_N = H_N^{-1}I_N + \sum_j a_j\Psi_{N,j} \qquad (9)$$

Each term in equation (9) can be characterized in the inertial range by a scaling exponent λ, defined by $f(br_i) = b^\lambda f(r_i)$. The exponents for the inhomogeneous solutions $H_N^{-1}I_N$ are given by simple dimensional analysis, $\lambda_N^{(I)} = N\gamma/2$, and agree with KOC theory. However for the zero modes of H_N, the scaling exponents are non-trivial and have to be determined as nonlinear eigenvalues along with $\Psi_{N,j}$ themselves. (The index j further enumerates the behaviour of Ψ under symmetries such as reflections, rotations and permutations.) Each of the terms in equation (9) varies with scale as $(r/L)^{\lambda_{N,j}}$ and hence, in the inertial range $r \gg L$, the term with the smallest positive

exponent dominates, so that the structure function exponent is $\zeta_N = \min\{\lambda_N^{(I)}, \lambda_{N,j}\}$. Anomalous scaling or intermittency corresponds to $\zeta_N < \lambda_N^{(I)}$. Modes other than the one with smallest positive λ define the rate at which all the details of the integral scales decay away within the inertial range. (Negative $\lambda_{N,j}$ also exist, and describe how the influence of dissipation or local source decays as r increases.) This "zero mode" mechanism of anomalous scaling was recognized and investigated independently in refs 18–20.

In identifying ζ_N with the dominant scaling exponent of C_N, we have tacitly used the fact that the moments of the structure function, S_N, can be obtained simply by 'fusing' points together. This can be demonstrated explicitly. Furthermore, whenever a pair of points get very close, say $\rho = r_{12}$ much less than all other r_{ij}, one finds from the local analysis using equation (7) that the ρ dependence of C_N follows $S_2(\rho)$ (refs 37, 39, 40). This allows the scaling of C_N to be related to the scaling of the correlators of dissipation at different points[37] providing a link between the Hopf equation approach and the traditional parametrization (since Kolmogorov's 1962 theory[10,11]) of intermittency[10] in terms of the fluctuations in the dissipation rate. However, it is not possible to circumvent the need for global solution of the $(N-1)$ d dimensional Hopf equation for C_N in computing the exponents by working with the structure function (depending on the single distance r). There is no closed equation with any of the $r_{ij} = 0$, as is evident in the path integral formulation: bringing the r_i observation points together, for example, $\langle\theta^N(r_1,t)\rangle$, does not eliminate the need to integrate over N distinct trajectories (now ending at the same r_1).

The Hopf equation ignores the temporal correlations of the velocity field, $\tau_r \approx r^{2/3}$ except in so far as they enter $D_{ab}(r)$. However at high Reynolds number fluid mechanics requires on average that $\tau_r \Delta_r V \approx r$, that is, the displacement of two points in one correlation time is of order their spacing. Thus, if one takes the $\tau \to 0$ limit while maintaining $\tau_r \Delta_r V \approx r$ scaling, the evolution equation (7) must be scale invariant and hence the scaling dimension of the H_N should be 0. Because temporal correlations are defined in a lagrangian frame, it is not possible to provide a simple gaussian model in eulerian coordinates analogous to equation (2). One approach is to eschew a model velocity field completely and model the Hopf operator directly, using symmetries and known limits as a guide[20,40]. A similar methodology has proved effective for the strong interactions in high-energy physics. Consequences of this approach are contained in the following section, but the discussion so far should already convince the reader that the scaling exponents for C_N do depend on the precise form of H_N, and thus in principle on more (or other) parameters than γ and d which were defined in equation (2).

Anomalous scaling

For general parameter values, analytic solution of equation (7) is hopeless; but by moving away from the physical regime ($d = 3$, $\gamma = 2/3$), perturbative expansions for exponents can be obtained, which definitively establish the intermittency corrections to KOC. Three limits have been explored: (1) the diffusion limit $2 - \gamma \ll 1$ (corresponding to a rough velocity field) studied by Gawedsky and Kupiainen[18]; (2) the large spatial dimension limit $d \gg 1$ of Chertkov *et al.*[19] and (3) the near-Batchelor limit $\gamma \ll 1$ (corresponding to a smooth velocity field) studied by Pumir and the authors[20,40,41]. In the former two limits the expansion is about a gaussian solution where the $2n$ point correlators factorize pairwise. The two limits can be combined into a single expression, $\zeta_{2n} - \zeta_{2n}^K = -2(2-\gamma)n(n-1)/(d+2) + o(2-\gamma)^2/d^2$. The nearly smooth field case, $\gamma \ll 1$, relies on the integrability of the Batchelor limit[20,40,42] resulting from the underlying high symmetry of H_N in that case. However, the dependence on small γ is non-analytic, and the required singular perturbation theory has only been performed for $N = 3$. The third moment, which appears in the presence of large-scale anisotropy, is the lowest correlator with non-trivial scaling: $\zeta_3 = 1 + o(\gamma^{3/2}) < \zeta_3^K = 1 + \gamma$. In the $2 - \gamma \ll 1$ limit[43], $\zeta_3 = \zeta_3^K - 2\gamma/5$ is also anomalous. Furthermore, Pumir[43,44] obtained a numerical solution of the Hopf equation for $N = 3$ (and all γ in $d = 2, 3$) yielding in particular $\zeta_3 = 1.38$ for the physically relevant case of $\gamma = 2/3$ and $d = 3$.

Frisch, Mazzino, Noullez and Vergassola[45] implemented the lagrangian path integral representation of equation (4) as a numerical Monte Carlo algorithm for solving equations (1) and (2), and calculated ζ_{2n} for C_{2n} by following $2n - 1$ points (the centre of mass is irrelevant) backwards in time. Results for $n = 2$ appear in Fig. 4. In addition, for a velocity field with realistic temporal correlations and $\gamma = 2/3$, it has been established[46] in two dimensions that the ζ_{2n} approach a constant value of 1.4 with increasing n. The saturation of the exponent would be expected if intermittency was due to front-like structures, and was predicted by the semi-classical analysis[47,48].

Returning to the third order moment, we note that it is interesting both as a lowest-order anomalous correlator and because its anomaly carries a clear physical significance: it indicates that the anisotropy which is always present on large scales finds its way to the small scales. Enforcing isotropy on the large scales does not eliminate this phenomenon, but merely requires a multi-scale correlator to make it visible again. Experiments in many geometries[7,8] quite generally find $\zeta_3 \approx 1$—a much stronger anomaly than the 1.38 found in the δ-correlated model. The disagreement is not altogether surprising given that, as we have

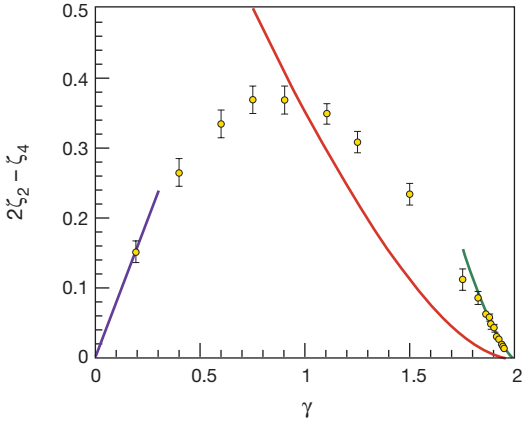

Figure 4 Anomalous scaling exponent, $2\zeta_2 - \zeta_4$, versus scaling index γ (see equation (2)). The structure function, was obtained from the lagrangian Monte Carlo simulation[45] of the Kraichnan model (circles) and is compared with analytic perturbation theory[18,41] of the Hopf equation (blue, green) and the prediction of the linear Ansatz[15] (red).

already remarked, the latter model does not properly capture the lagrangian correlation and that the scaling exponents are non-universal eigenvalues which depend on the details of the evolution operator H_N. The class of phenomenological evolution operators introduced in ref 20 allows for stronger intermittency. The theory also produces a prediction for the full configuration dependence of $C_3(r_1,r_2,r_3)$ which has been compared to the experimental measurements in a wind tunnel[25] (with an imposed temperature gradient). The configuration dependence of C_3 is the simplest measure of the 'geometry' of the intermittent structures. Figure 5 illustrates how the contribution (to C_3) of randomly distributed, but preferentially oriented, fronts depends on the geometry of the triangle (within a naive model where the fronts are sharp, straight and of unitary height). To the extent that $\zeta_3 \approx 1$ (expected if the fronts are sharp and unitary), and the configuration dependence based on the 'naïve' model qualitatively conforms with the observation, the front interpretation stands. Yet both the explicit calculation C_3 and the observation[25] exhibit quantitative deviations from the simple front model, indicating that the height of the fronts, their width and spatial extent all have non-trivial distribution[46].

Higher multipoint correlators of θ and $\partial\theta$ can be used to study the latter in detail. It would be particularly interesting to examine the four-point correlator $\langle\partial\theta(r_1)\partial\theta(r_2)\partial\theta(r_3)\partial\theta(r_4)\rangle$. If the fluctuations are dominated by sheets, this four-point object should be maximal when the points are coplanar[49]. The decay of the correlator as one of the points leaves the plane would quantify the width of the sheets which may be expected to depend on the scale, controlled by the separation of the other three points.

Lessons of scalar turbulence

The study of nonequilibrium problems has lagged behind systems in thermal equilibrium because there is no way, analogous to averaging over the Boltzmann distribution, to compute equal time averages. Equilibrium statistical mechanics would be a very different subject if it were necessary to time-average solutions to Newton's equations. Thus, the recent progress in understanding passive scalar turbulence was grounded on the computationally useful representation of the stationary statistics. The lagrangian path integral formulation mapped the problem into statistical mechanical form. The Hopf equation (7) made possible systematic perturbative calculations of the multipoint correlators. Qualitatively new is the mechanism for generating anomalous scaling via zero modes of the Hopf operator which associates intermittency effects with the existence of statistically stationary unforced solutions in the inertial range. The operator is inherently multidimensional, and the statistics of the multipoint configurations are essential to understand intermittency. The theory naturally allows for an infinity of subdominant exponents that parametrize how all manner of large-scale anisotropies decay away in the inertial range. There is good evidence that the anomalous scaling exponents reach saturation for large N as would be the case with sharp unitary fronts dominating large fluctuations as in Burger's "turbulence"[10].

Exponents appear as nonlinear eigenvalues, and thus depend on all details of the velocity statistics embodied in the Hopf operator. This dependence on the velocity ensemble makes the exponents for passive scalar turbulence non-universal, and unless the statistics of the turbulent velocity itself proves to be fully universal (that is, independent of the forcing and boundary conditions) in an experimentally attainable regime, this lack of universality should manifest itself in observations.

The lagrangian path integral representation has provided both a useful analytic tool and a new numerical simulation approach. It has been used to produce considerable analytic insight into dissipation statistics[37] and into the nature of the direct and inverse cascade[50], as well as a reliable numerical calculation of the structure function exponent[45,46]. Also significant is the emergence of the $1/d$ expansion[19] in the context of turbulence[51]. The most immediate application for these tools is in the context of the magnetic dynamo problem[34,49], where the amplification of the magnetic field vector is in a certain way analogous to the behaviour of the passive scalar gradient.

It is useful to contrast passive scalar turbulence with critical phenomena at second-order phase transitions[52], as both problems exhibit scale-invariant correlations. The obvious distinction is that the scaling behaviour in turbulence is confined to inertial scales ($r < L$) and the correlations grow with r/L rather then decrease at long distance as in critical phenomena. The universality in critical theories is embodied by the fixed-point equation for the effective free energy at long wavelength, and that only two exponents suffice to determine all the others. Scaling exponents are additive as long as the fields entering the correlator are not at the same point and develop 'anomalies' when the observation points are fused. Curiously, the situation is opposite for the passive scalar, where addition of an observation point to a correlator picks up a new, higher-order exponent, whereas points fuse with impunity.

The lessons and methods of the passive scalar problem have implications for hydrodynamic turbulence, even though the defining equations are no longer linear. Subgrid modelling or Reynolds stress closures which seek to parametrize the unresolved small scales have a long history in turbulence modelling[11], and multipoint correlators might point to better representation of the interactions between scales. Furthermore, the tendency towards the formation of structures for the passive scalar may be robust enough to carry over to the velocity field. In particular, scalar gradient sheets and their alignment with the large-scale gradient may have an analogue in the transient appearance of vortex sheet structures in shear flow[53,54]. The latter would result in the persistence of anisotropy on small scales which becomes only stronger for higher-order moments.

Ultimately, the most significant lesson of the passive scalar problem is the fundamental importance of the multipoint correlators. The configuration dependence of C_N is both measurable and dynamically significant. Prior work on turbulence concentrated on either two-point statistics and its scaling or on 'snapshots' of the velocity or scalar fields and identification of spatial 'structures'. Multipoint correlators naturally fill the gap between the two approaches; they provide new, physically interesting observables for the experiments and direct numerical simulations, and ultimately new prospects for the quantitative understanding of turbulence. □

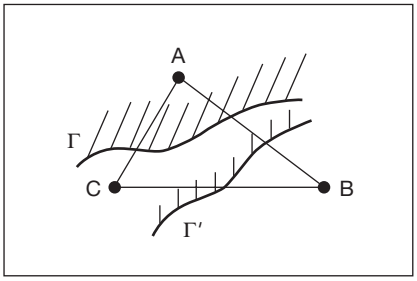

Figure 5 Contribution of fronts and configuration dependence of the three-point correlator. If Γ and Γ' are fronts separating $\theta = 1$ from $\theta = -1$, the former contributes +1 to the C_3 correlator, while the latter contributes −1. The resulting value of C_3 depends on the shape of the ABC triangle.

1. Pasquill, F. & Smith, F. B. *Atmospheric Diffusion* (Ellis Horwood, Chichester, 1983).
2. Dibble, R. W., Warnatz, J. & Maas, U. *Combustion: Physical and Chemical Fundamentals, Modelling and Simulations, Experiments, Pollutant Formation* (Springer, New York, 1996).
3. Proctor, M. R. E. & Gilbert, A. D. (eds) *Lectures on Solar and Planetary Dynamos* 117 (Cambridge Univ. Press, Cambridge, 1994).
4. Berg, H C. Bacterial microprocessing. *Cold Spring Harbor Symp. Quant. Biol.* **55,** 539–545 (1990).
5. Atema, J. Chemical signals in the marine environment: dispersal, detection, and temporal signal analysis. *Proc. Natl Acad. Sci.* **92,** 62–66 (1995).

6. Mafraneto, A. & Carde, R. T. Fine-scale structure of pheromone plumes modulates upwind orientation fo flying moths. *Nature* **369,** 142–144 (1994).
7. Sreenivasan, K. R. On local isotropy of passive scalars in turbulent shear flows. *Proc. R. Soc. Lond. A* **434,** 165–182 (1991).
8. Warhaft, Z. Passive scalars in turbulent flows. *Annu. Rev. Fluid Mech.* **32,** 203–240 (2000).
9. Sreenivasan, K. & Antonia, R. A. The phenomenology of small scale turbulence. *Annu. Rev. Fluid Mech.* **29,** 435–472 (1997).
10. Frisch, U. *Turbulence: The legacy of AN Kolmogorov* (Cambridge Univ. Press, Cambridge, 1995).
11. Monin, A. S. & Yaglom, A. M. *Statistical Fluid Mechanics* (MIT Press, Cambridge, 1975).
12. Tennekes, H. & Lumley, J. A. *First Course in Turbulence* (MIT Press, Cambridge, 1972).
13. Edouard, S. *et al*. The effect of small-scale inhomogeneities on ozone depletion in the Arctic. *Nature* **384,** 444–447 (1996).
14. Kraichnan, R. H. Small-scale structure of a scalar field convected by turbulence. *Phys. Fluids* **11,** 945 (1968); Convection of a passive scalar by a quasi-uniform random straining field. *J. Fluid Mech.* **64,** 737–762 (1974).
15. Kraichnan, R. H. Anomalous scaling of a randomly advected passive scalar. *Phys. Rev. Lett.* **72,** 1016–1019 (1994).
16. Holzer, M. & Siggia, E. D. Turbulent mixing of a passive scalar. *Phys. Fluids* **6,** 1820–1837 (1994).
17. Pumir, A. A numerical study of the mixing of a passive scalar in 3 dimensions in the presence of a mean gradient. *Phys. Fluids* **6,** 2118–2132 (1994).
18. Gawcedzki, K. & Kupiainen, A. Anomalous scaling of the passive scalar. *Phys. Rev. Lett.* **75,** 3834–3837 (1995).
19. Chertkov, M., Falkovich, G., Kolokolov, I. & Lebedev, V. Normal and anomalous scaling of the fourth-order correlation function of randomly advected passive scalar. *Phys. Rev. E* **52,** 4929–4941 (1995).
20. Shraiman, B. I. & Siggia, E. D. Anomalous scaling of a passive scalar in a turbulent flow. *C.R. Acad. Sci.* **321,** 279–284 (1995).
21. Antonia, R. A. & van Atta, C. W. Structure functions of temperature fluctuations in turbulent shear flows. *J. Fluid Mech.* **84,** 561–580 (1978).
22. Gibson, C., Freihe, C. & McConnell, S. Structure of sheared turbulent fields. *Phys. Fluids* **20,** S156–S167 (1977).
23. Mestayer, P. G. Local isotropy and anisotropy in a high-Reynolds-number turbulent boundary layer. *J. Fluid Mech.* **125,** 475–503 (1982).
24. Jayesh & Warhaft, Z. Probability distributions of a passive scalar in grid generated turbulence. *Phys. Rev. Lett.* **67,** 3503–3506 (1991).
25. Mydlarsky, L., Pumir, A., Shraiman, B. I., Siggia, E. D. & Warhaft, Z. Structure and multi-point correlators for turbulent advection. *Phys. Rev. Lett.* **81,** 4373–4376 (1998).
26. Gollub, J. P., Clarke, J., Gharib, M., Lane, B. & Mesquita, O. N. Fluctuations and transport in a stirred fluid with a mean gradient. *Phys. Rev. Lett.* **67,** 3507–3511 (1991).
27. Ottino, J. M. *The Kinematics of Mixing: Stretching, Chaos, and Transport* (Cambridge Univ. Press, New York, 1989).
28. Ott, E. *Chaos in Dynamical Systems* (Cambridge Univ Press, New York, 1994).
29. Williams, B. S., Marteau, D. & Gollub, J. P. Mixing of a passive scalar in magnetically forced two-dimensional turbulence. *Phys. Fluids* **9,** 2061–2080 (1997).
30. Miller, P. L. & Dimotakis, P. E. Measurements of scalar power spectra in high Schmidt number turbulent jets. *J. Fluid Mech.* **308,** 129–146 (1996).
31. Chen, S. & Kraichnan, R. H. Simulations of a randomly advected passive scalar field. *Phys. Fluids* **68,** 2867–2884 (1998).
32. Feynman, R. & Hibbs, A. *Quantum Mechanics and Path Integrals* (McGraw Hill, New York, 1965).
33. Drummond, I. T. Path-integral for turbulent diffusion. *J. Fluid Mech.* **123,** 59–68 (1982).
34. Molchanov, S., Ruzmaikin, A. & Sokolov, A. Kinematic dynamo. *Sov. Phys. Usp.* **28**, 307–327 (1985).
35. Shraiman, B. I. & Siggia, E. D. Lagrangian path integrals and fluctuations in random flow. *Phys. Rev. E* **49,** 2912–2927 (1994).
36. Bernard, D., Gawedzki, K. & Kupiainen, A. Slow modes in passive advection. *J. Stat. Phys.* **90,** 519–569 (1997).
37. Chertkov, M., Falkovich, G. & Kolokolov, I. Intermittent dissipation in PS turbulence. *Phys. Rev. Lett.* **80,** 2121–2124 (1998).
38. Buck, K. A. & Dahm, W. J. A. Experimental study of the fine scale structure of conserved scalar mixing in turbulent shear flows. Part I. Sc $\gg$ 1. *J. Fluid Mech.* **317,** 21–71 (1996).
39. Fairhall, A., Gat, O., L'vov, V. & Procaccia, I. Anomalous scaling in a model of passive scalar advection. *Phys. Rev. E* **53,** 3518–3535 (1996).
40. Shraiman, B. I. & Siggia, E. D. Symmetry and scaling of turbulent mixing. *Phys. Lett.* **77,** 2463–2466 (1996); Anomalous scaling of passive scalar near Batchelor limit. *Phys. Rev. E* **57,** 2965–2977 (1998).
41. Pumir, A., Shraiman, B. I. & Siggia, E. D. Perturbation theory for the δ-correlated model of passive scalar advection near the Batchelor limit. *Phys. Rev. E* **55,** R1263–R1266 (1997).
42. Balkovsky, E., Chertkov, M., Kolokolov, I. & Lebedev, V. 4-th order correlation fucntion of a randomly advected passive scalar. *JETP Lett.* **61,** 1049–1054 (1995).
43. Pumir, A. Anomalous scaling behaviour of a passive scalar in the presence of a mean gradient. *Europhys. Lett.* **34,** 25–29 (1996).
44. Pumir, A. Structure of the three-point correlation function of a passive scalar in the presence of a mean gradient. *Phys. Rev. E* **57,** 2914–2929 (1998).
45. Frisch, U., Mazzino, A., Noullez, A. & Vergassola, M. Lagrangian method for multiple correlations in passive scalar advection. *Phys. Fluids.* **11,** 2178–2186 (1999).
46. Celani, A., Lanotte, A., Mazzino, A. & Vergassola, M. Universality and saturation of intermittency in passive scalar turbulence. *Phys. Rev. Lett.* **84,** 2385–2388 (2000).
47. Chertkov, M. Instanton for random advection. *Phys. Rev. E* **55,** 2722–2735 (1997).
48. Balkovsky, E. & Lebedev, V. Instanton for the Kraichnan random advection model. *Phys. Rev. E* **58,** 5776–5795 (1998).
49. Chertkov, M., Falkovich, G., Kolokolov, V. & Vergassola, M. Small scale magnetic dynamo. *Phys. Rev. Lett.* **83,** 4065–4068 (1999).
50. Chertkov, M., Kolokolov, L., Vergassola, M. Inverse versus direct cascades in turbulent advection. *Phys. Rev. Lett.* **80,** 512–515 (1998).
51. Fournier, J.-D., Frisch, U. & Rose, H. Infinite-dimensional turbulence. *J. Phys. A* **11**, 187–198 (1978).
52. Wilson, K. G. The renormalization group and critical phenomena. *Rev. Mod. Phys.* **55,** 583–600 (1983).
53. Pumir, A. & Shraiman, B. I. Persistent small scale anisotropy in homogeneous shear flows. *Phys. Rev. Lett.* **75,** 3114–3117 (1995).
54. Warhaft, Z. & Garg, S. On the small scale structure of simple shear flow. *Phys. Fluids* **10,** 662–673 (1998).

Acknowledgements

The authors have greatly benefited from interactions with colleagues, and are particularly grateful to S. Chen, K. Sreenivasan, P. Tabeling, Z. Warhaft and L. Mydlarski for contributing to the figures.